The effect of copper and cerium infiltration on LSM Cathode microstructure in solid oxide fuel cells

Maryam Irandoost[1] | Niloofer Afshar[1] | Pirooz Marashi[1] | Zahra Sadeghian[2, *]

[1]Department of Materials and Metallurgical Engineering, Amirkabir University of Technology, Tehran, Iran

[2]Research Institute of Petroleum Industry (RIPI), Tehran, Iran, Email: sadeghianz@ripi.ir

Abstract

Solid oxide fuel cells are a technology that can convert chemical energy directly into electrical energy. In the present study, single-phase lanthanium strontium manganate (LSM) nanoparticles with the nominal chemical formula $La_{0.8}Sr_{0.2}MnO_3$ were successfully synthesized by the improved Pechini method. The infiltration of heterogeneous copper and cerium electrocatalysts on the cathode was investigated. X-ray diffraction (XRD) was used to determine the phase composition. The microstructure and surface morphology of the synthesized powder was characterized using a scanning electron microscope (SEM). The coated composition was examined using energy dispersive spectroscopy (EDS) and elemental mapping images. The microstructure of the electrocatalysts seeded on the cathode was studied by FE-SEM. The infiltration of 0.5 M copper + 0.5 M cerium nanoparticles (dimensions from 23 to 52 nm) with a broad distribution on the LSM cathode surface was obtained. Results showed that using single-component solutions of copper and cerium nanoparticles with dimensions of 39-61 nm and 20-42 nm, respectively, were generated on the cathode surface. The formation of agglomerated particles was observed as the cerium solution concentration increased. Secondary copper growth was observed as the copper solution concentration increased.

1. Introduction

Solid oxide fuel cells generate electricity with advantages such as no pollution, high efficiency of more than 70%, and relatively low cost [1]. Due to their ceramic components, solid oxide fuel cells have high operating temperatures [2]. The best-known high-temperature fuel cell cathode is a perovskite-based lanthanumcontaminated manganese, such as lanthanum strontium manganite (LSM). Due to its high electrical conductivity, this cathode shows good performance and chemical compatibility with two well-known electrolytes, yttria-stabilized zirconia (YSZ) and gadolinium-doped series (GDC) [3]. The resistance of the cathode and the electrical conductivity are responsible for the ohmic loss in a solid oxide fuel cell. The LSM-YSZ cathode is the most widely used electrode in fuel cells [4]. Adding an electrocatalyst to the surface of the cathode is one method used to stabilize its electrochemical activity [5]. There are different types of electrocatalysts, including precious metals, such as palladium and platinum; iron-conducting oxides, such as samarium and gadoliniumdoped ceria family (SDC and GDC, respectively); and both ion- and electronconducting catalysts, such as strontiumdoped samariumcobaltite (SSC), nonionic, and electronic oxides such as copper or calcium oxides and multiphase catalysts [6].

Heterogeneous perovskite electrocatalysts include LSCF, LSF, LSM, and other perovskite families. Electrocatalysis is heterogeneous catalysis using spectroscopy techniques. It offers specific information about the reaction process at the gas/solid interface, in contrast to the more complex system conducted at the triple-phase interfaces of electrocatalysts, where reactant, electron, and active sites are related. Heterogeneous electrocatalysts have been shown to accelerate reactions by activating active sites at the three-phase interphases [7-9]. For example, Lou et al. examined the porous LSM-YSZ cathode with some samarium-infiltrated SSC. The size of the SSC particles that penetrated the cathode surface was 2080 nm, and they appear to be well attached to the pore walls of the LSM-YSZ network; however, most of the particles were separated. They reported that the cell performance improvement comes from the improvement of the LSM-YSZ cathode after the addition of the SSC nanoparticle.

Another study found that the Polarization resistance was reduced by performing an electrochemical impedance analysis [10]. Moreover, a study by Pinging et al. observed that infiltration sequencing of SSC and SDC had an impact on the morphology and performance of the LSM oxygen electrode; this effect decreased as the infiltration duration increased [11]. They found that the SDC particles with a grain size of about 10 nm were evenly dispersed on the LSM grains, whereas the LSM-SSC electrode showed a distinct morphology, and SSC particles between 40 and 50 nm were produced [11].

Alkali earth metal compounds and transition metal oxides such as calcium, magnesium, copper, and cerium oxides have been used for infiltration in porous cathodes and composite materials. These oxides have low electrocatalytic activity compared to other infiltration materials, and inactive oxide must be coated as separate particles rather than uniform particle coating; otherwise, they will block oxygen reduction reaction (ORR) reactions [6, 12]. Nanoparticles are formed by infiltration, in which a precursor solution is applied on a porous scaffold and then heat treated to create evenly distributed particles. To infiltrate a scaffold, one typically drips the infiltration solution onto the target substrate, allows the solution to dry to extract the solvent, and then sinters the infiltrated structure to create the required crystalline structures. Ideally, the infiltrated structure shows a consistent nanoparticle distribution throughout the intended scaffold [13, 14]. One of the

face, while other studies showed that silver and ceria concurrent infiltration improves cathode performance [18, 19].

The aim of the present study was to synthesize LSM and determine the influence of the concentration of the infiltration solution on the morphology. For the ORR reaction, cerium is used as a ceramic electrocatalyst and copper as a metallic electrocatalyst. At intermediate SOFC temperatures, doped CeO_2 is commonly used as the ion-conducting infiltrate material due to its larger oxide ionic conductivity coefficient compared to conventional cathode materials such as LSM. Simultaneous and separate infiltration of solutions of copper and ceria electrocatalysts at concentrations of 0.5 M and 1 M as well as simultaneous infiltration of 0.5 M cerium + 0.5 M copper, are studied.

2. Experimental

2.1. Preparation of the LSM powder

To evaluate the formation of copper oxide nanoparticles on the LSM cathode, the LSM powder was first synthesized. The synthesis of the cathode powder with a stoichiometric ratio of $La_{0.8}Sr_{0.2}MnO_3$ was done according to the Pechini method [20]. The starting materials were lanthanum nitrate $(La(NO_3)_3 \cdot 6H_2O)$ (>99.0%, Merck), strontium nitrate $(Sr(NO_3)_2)$ (>99.0%, Merck), manganese nitrate $(Mn(NO_3)_2)$ (>98.5%, Merck), citric acid $(C_6H_8O_7)$, ethylene glycol $(C_2H_6O_2)$, and distilled water. The desired amount of product (x) was determined, and according to the formula, the mass of the reactant salts was calculated using the molar mass of each salt. Citric acid was added to the solution as a complexing agent, while polyethylene glycol was used as a surfactant. First, nitrates of metals were added to a certain amount of deionized water, and then citric acid was added to the solution. After exposing

advantages of this process is the ability to use expensive electrocatalysts sparingly and inexpensively since the amount of electrocatalyst that enters this process is much less than the amount of material used in the conventional cathode fabrication process. In addition, electrocatalysts with a high propensity to react with other cell components can be manufactured through a diffusion process incompatible with current production methods. Finally, the infiltration method produces scaffolds in the nanometer range that can be used for their nanometer properties [14].

Hong et al. studied copper inoculation on the LSCF cathode [15]. This study revealed that copper oxide nanoparticles with a size of 40 nm developed on the porous LSCF cathode and showed that a CuO-coated LSCF electrode surface could significantly improve ORR activity. They found that an enhanced surface exchange had a nonlinear relationship with respect to the CuO porous structure and the LSCF-CuO phase size, indicating that the enhanced oxygen reductions occurr at both the CuO-LSCF air interface and the CuO surface. Moreover, these particles drastically reduced the low-frequency resistance associated with the surface reaction mechanism [15].

Another study by Gao et al. showed that infiltration of a LSCF/CGO composite cathode with Cu nitrate solutions and generation of CuO nanoparticles successfully reduced the long- and short-term polarisation resistance of the cathode [16]. They reported that the improvement in cathode catalytic property by CuO infiltration before aging might be due to the dispersion of Cu^{2+} in the LSCF structure, leading to the formation of novel Cu-containing compounds such as LSCo-CuFe, thus, allowing an improvement in overall activation polarisation errors [16]. Furthermore, Tan et al. showed that the simultaneous inoculation of PdO and ZrO_2 catalysts significantly improved the LSM-YSZ cathode performance [17]. Two more studies showed that silver infiltration leads to agglomeration and non-uniform distribution of silver on the LSM cathode sur-

the solution to 80 °C for 1 hour, ethylene glycol was added, maintained at 80 ° C, then heated to 120 and 250 °C for 1 to 2 hours. Finally, LSM powder was calcined at 800 °C for 5 hours.

2.2. Production of the half-cell

The half-cell was manufactured with an anode and electrolyte using the tapecasting process. For this purpose, YSZ8 and YSZ8-NiO powder were mixed with solvent, binder, and plasticizer in a ball mill for 48 h. The electrolyte slurry was cast onto Mylar sheets and after drying the electrolyte layer, the anode slurry was cast onto this dried electrolyte layer at room temperature. Then the half-cell was heated at 1000 °C for 2 h for presintering and then sintered at 1450 °C for 3 hours. Next, the synthesized LSM powder was mixed with ethanol and an ink vehicle (a solvent and organic material such as terpineol) by ball milling for 2 h to form a slurry. Finally, the slurry was manually applied (painted) onto the electrolyte and sintered at 1200 °C for 2 h.

2.3. Infiltration

Copper and cerium nitrate were used to prepare the infiltration solution. A cerium precursor was used to form the seria, copper precursors were used to form the copper catalytic species, and ethanol was used to make the solvents. Depending on the volume of the volumetric balloons used in the dissolution procedure, the stoichiometric amount of metal salt was dissolved in a water and ethanol solvent at a volume ratio of water to ethanol of 4:6. The prepared solution concentrations were 0.5 M and 1 M using copper nitrate and cerium nitrate precursors [16]. The specification of the infiltration solutions in LSM cathodes is shown in Table 1. In order to determine the phase produced, the powder sample resulting from the synthesis process was analyzed by X-ray powder diffraction (XRD) using a PANalytical B.V. XRP machine model X'Pert PRO MPD. TESCAN's FE-SEM MIRA3 model was used to evaluate the microstructure of the samples by scanning the powder sample and determining the failure level of the fuel cell samples. EDS was performed for the elemental analysis of the samples. Elemental mapping was also performed on the samples.

Table.1. The specification of infiltration solutions in LSM cathodes.

Sample	Infiltration solutions
1	M Ce 0.5
2	M Ce 1
3	M Cu 0.5
4	M Cu 1
5	M Cu / 0.5 M Ce 0.5
6	M Cu / 1 M Ce 1

3. Results and discussion

The X-ray diffraction pattern of the synthesized LSM cathode (see Figure 1) is in good agreement with standard XRD data ICDD # 1043-011-98. The morphology of the synthesized LSM cathode powder was examined by FE-SEM. As can be seen in Figure 2, a homogeneous LSM powder with particle agglomeration can be seen in some places in the image. The dimensions of these particles are 35 to 89 nm. EDS and elemental mapping of the LSM powder analysis show the presence of lanthanum, strontium, and manganese. Figures 3 and 4 show the FE-SEM images of the cross-section sample cathode after infiltration with 0.5 M and 1 M Ce and Cu, respectively. As can be seen in Figure 3, the EDS spectrum in LSM infiltrated with 1 M Cu has a higher peak compared to that with 0.5 M Cu. In Figure 4, cerium particles are placed in

a homogeneous layer on the surface of the cathode such that the particle size was approximately 2042 nm at both concentrations. The particle size is about 20 to 42 nm for both concentrations. The distribution of 0.5 M cerium nanoparticles on the cathode is more homogeneous than 1 M Ce because solutions with lower concentration and viscosity have higher diffusion resulting in a uniform distribution of electrocatalytic nanoparticles. Therefore, the microstructure of the catalyst layer on the cathode surface depends on the metal concentration in the infiltration solutions and the infiltration method to help minimize the resistance to the ORR at the cathode. Cathode impregnation improves performance and efficiency [14].

Figure 5 shows the microstructure of copper and cerium particles with different concentrations on the cathode surface. Preliminary substances containing 0.5 M copper plus 0.5 M cerium and 1 M copper plus 1 M cerium were used for infiltration onto the LSM cathode. The particle distribution on the cathode surface close to the electrolyte-cathode interface is visible. Despite the different particles, the particle distribution is not uniform, which may be related to the high cerium concentration, resulting in an agglomerated particle solution and secondary copper growth due to the increase in the copper solution.

In a study by Seyed-Vakili et al. [19], a comparison between the combined and individual effects of ceria and silver infiltration on the LSM cathode showed the benefit of the combined infiltration of these two electrocatalysts. Ceria infiltration has also been shown to be effective in reducing silver particle agglomeration over long periods of operation [20]. In another study [21], the effect of strontium-doped cerium showed that the cerium oxide nanoparticles on the surface of the LSM-YSZ cathode interface caused a higher concentration of strontium at the LSM-YSZ interface. In an infiltration study, ceria and cobalt nanoparticles were simultaneously inoculated onto the LSM-YSZ cathode, and it was found that cerium oxide particles prevent the aggregation of nanoparticle cobalt oxide in the cathode microstructure [22].

In our study, the simultaneous infiltration of cerium and copper at a concentration of 0.5 M gave the best results. As noted in previous research, the addition of cerium to materials such as cobalt avoids copper agglomeration. It was expected that nfiltrating a phase with higher oxide ionic would significantly improve the performance od LSM-based cathodes since the poor ionic oxygen conductivity of LSM limits the ORR response to areas close to TBP.
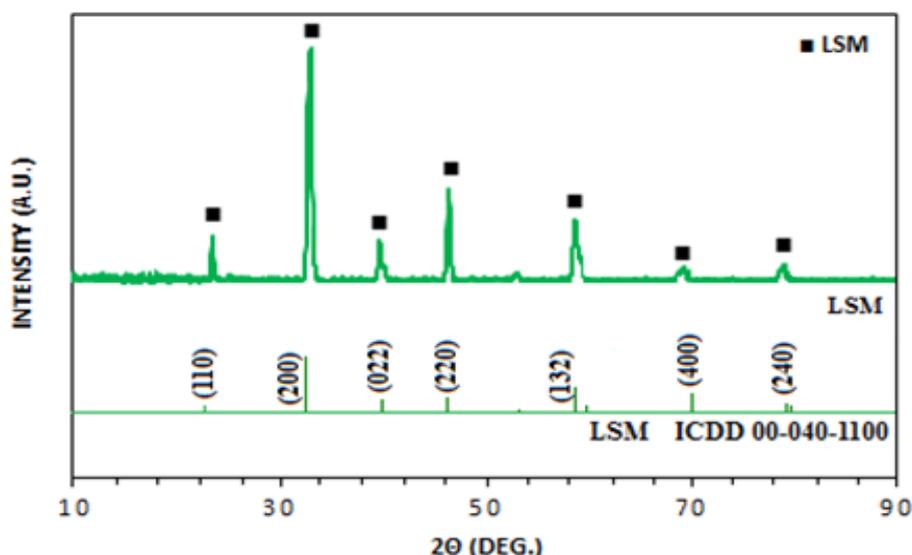
Fig. 1. XRD patterns of LSM synthesized powders.
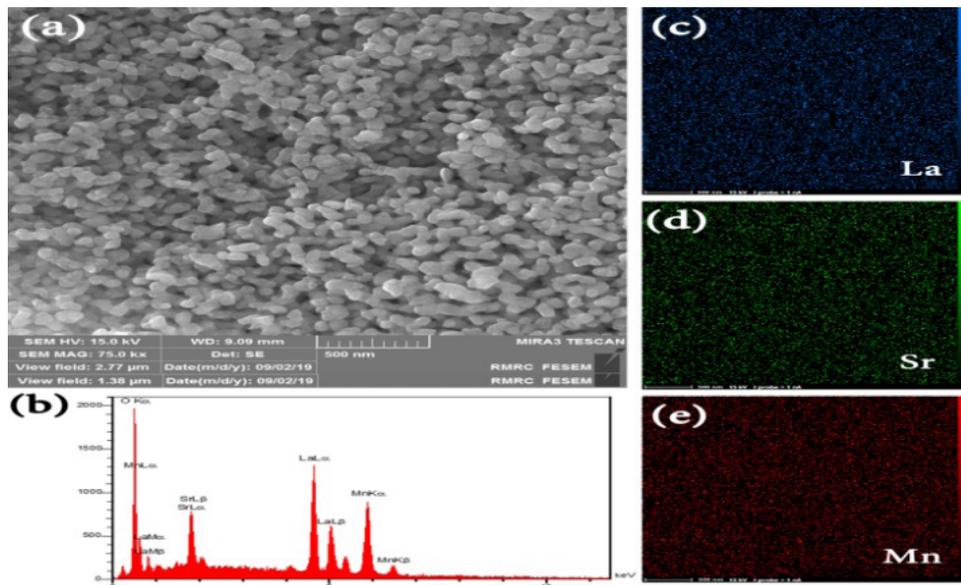
Fig.2. (a) FE-SEM images of synthesized LSM powder, (b) EDS spectrum of LSM, and (c-e) elemental mapping images of La, Sr, and Mn, respectively.
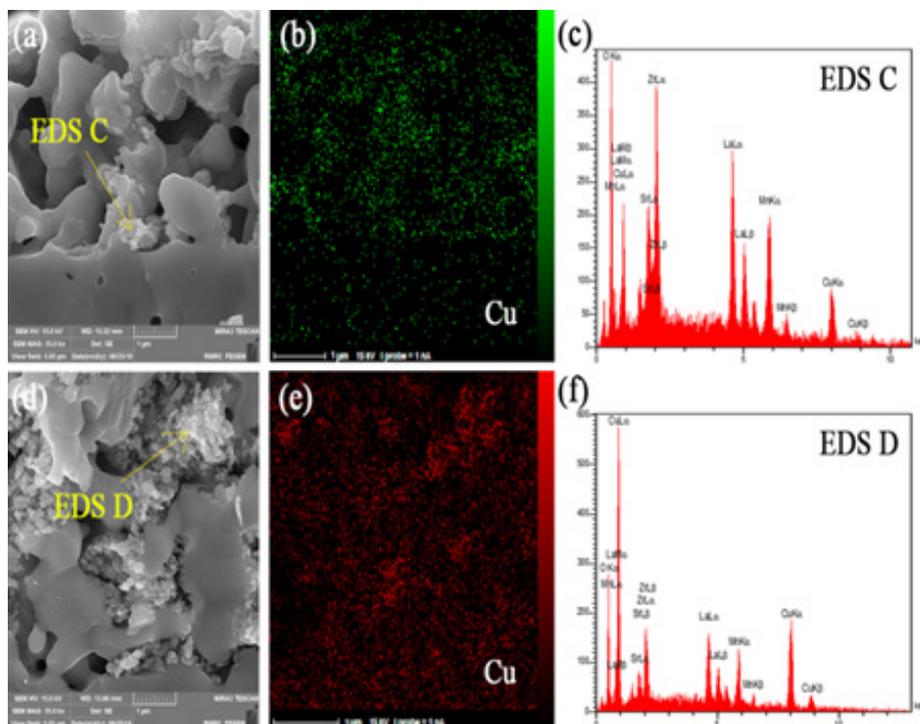
Fig. 3. (a,d) FE-SEM images of an infiltrated sample containing 0.5M Cu and 1M Cu, (c,f) EDS spectrum of infiltrated samples, and (b,e) elemental mapping images of 0.5M Cu and 1M Cu, respectively.
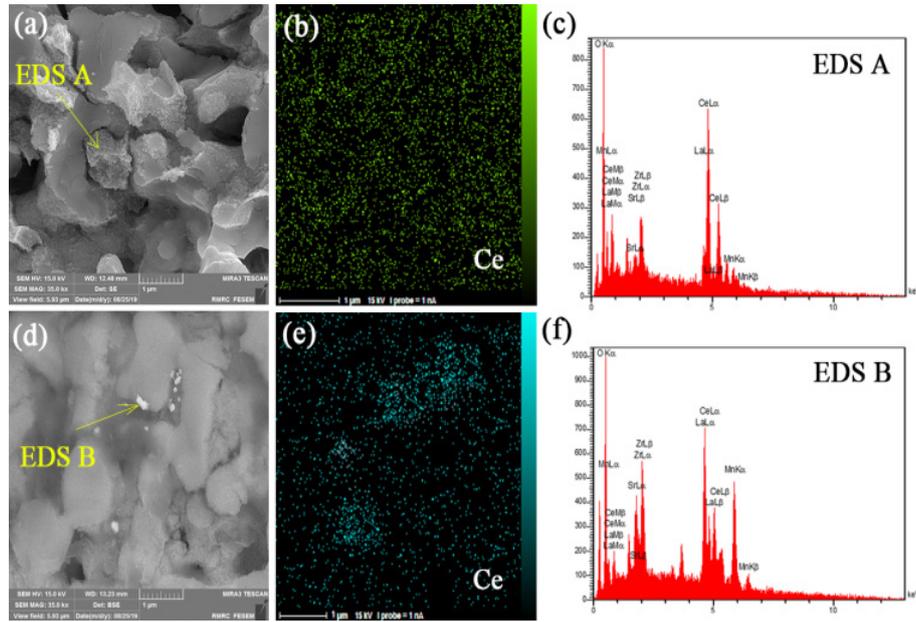
Fig. 4. (a,d) FE-SEM images of an infiltrated sample containing 0.5M Ce and 1M Ce, (c,f) EDS spectrum of infiltrated samples, and (b,e) elemental mapping images of 0.5M Ce and 1M Ce, respectively.
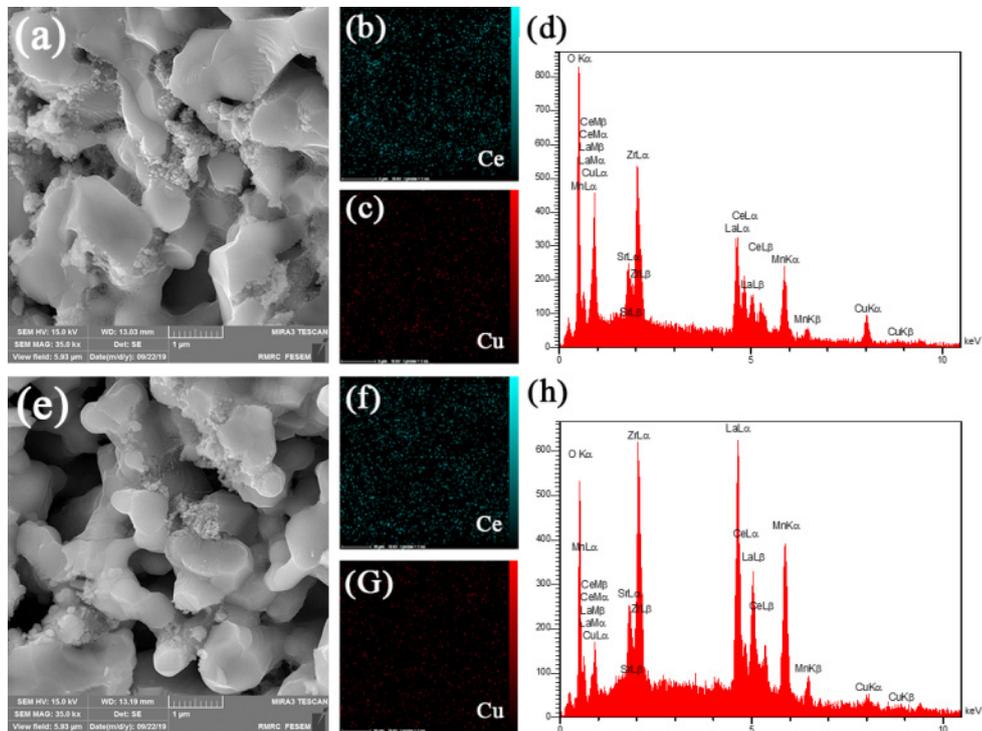
Fig. 5. (a,e) FE-SEM images of infiltrated samples with (0.5M Cu+0.5M Ce) and (1M Cu+1M Ce), (d,h) EDS spectra of infiltrated samples, and (b,c,f,g) elemental mapping images of (0.5M Ce+0.5M Cu) and (1M Ce + 1M Cu), respectively.

Conclusion

The LSM cathode in the solid oxide fuel cell was synthesized by the Pechini method. Copper and cerium are cheap and simple heterogeneous electrocatalysts compared to other catalysts used in solid oxide fuel cells. The role of cerium was to prevent agglomeration and non-accumulation of particles at the same time as copper infiltration. Infiltration of nanocomponent cerium solutions at both concentrations produced a thin layer of cerium nanoparticles between 20 nm to 42 nm. Infiltration of nanocomponent copper solutions at both concentrations mainly produced an uneven distribution of nanoparticles with dimensions from 39 nm to 61 nm on the surface. Copper nanoparticles with relatively small sizes between 20 and 42 nm after infiltration of 0.5 M cerium solution did not form agglomerate particles with the 1 M solution, and the resulting smaller nanoparticles were between 17 and 61 nm. The 1 M cerium solution yielded a particle size between 42 and 72 nm. Therefore, these concentrations were chosen as the most suitable for the simultaneous co-penetration of heterogeneous copper and cerium electrocatalysts. The infiltration of 0.5 M Cu + 0.5 M Ce solution had the higher penetration among the two-component copper and cerium solutions and generated nanoparticles with a broad distribution on the LSM surface between 23 nm to 52 nm.

References

[1] Z. Zakaria, S.H. Abu Hassan, N. Shaari, A.Z. Yahaya, Y. Boon Kar, (2020) .A review on recent status and challenges of yttria stabilized zirconia modification to lowering the temperature of solid oxide fuel cells operation, *International Journal of Energy Research* 44(2) 631-650.

[2] M. Ghamarinia, A. Babaei, C. Zamani, (2020). Electrochemical characterization of La2NiO4-infiltrated La0. 6Sr0. 4Co0. 2Fe0. 8O3-δ by analysis of distribution of relaxation times, *Electrochimica Acta* 353 ,136520.

[3] Z. Zakaria, Z. Awang Mat, S.H. Abu Hassan, Y.J.I.J.o.E.R. Boon Kar ,(2020). A review of solid oxide fuel cell component fabrication methods toward lowering temperature, 44(2) 594-611.

[4] O. Agbede, K. Hellgardt, G. Kelsall. (2020). Electrical conductivities and microstructures of LSM, LSM-YSZ and LSM-YSZ/LSM cathodes fabricated on YSZ electrolyte hollow fibres by dip-coating, *Materials Today Chemistry* 16 , 100252.

[5] E. Dogdibegovic, R. Wang, G.Y. Lau, M. Tucker, High performance metal-supported solid oxide fuel cells with infiltrated electrodes, *Journal of Power Sources* 410 (2019) 91-98.

[6] Y. Niu, W. Huo, Y. Yu, W. Li, Y. Chen, W. Lv. (2022). Cathode infiltration with enhanced catalytic activity and durability for intermediate-temperature solid oxide fuel cells, *Chinese Chemical Letters* 33(2) ,674-682.

[7] J.M. Vohs, R.J. Gorte. (2009). High-performance SOFC cathodes prepared by infiltration, *Advanced Materials* 21(9) , 943-956.

[8] A. Yazdani, G.G. Botte. (2020). Perspectives of electrocatalysis in the chemical industry: a platform for energy storage, *Current Opinion in Chemical Engineering* 29 , 89-95.

[9] J. Yu, R. Ran, Y. Zhong, W. Zhou, M. Ni, Z. Shao. (2020). Advances in porous perovskites: synthesis and electrocatalytic performance in fuel cells and metal–air batteries, *Energy & Environmental Materials* 3(2) 121-145.

[10] C. Lu, T.Z. Sholklapper, C.P. Jacobson, S.J. Visco, L.C. De Jonghe. (2006). LSM-YSZ cathodes with reaction-infiltrated nanoparticles, *Journal of the Electrochemical Society* 153(6) , A1115.

[11] P. Wu, Y. Tian, Z. Lü, X. Zhang, L. Ding. (2022) .Electrochemical performance of La0. 65Sr0. 35MnO3 oxygen electrode with alternately infiltrated Sm0. 5Sr0. 5CoO3-δ and Sm0. 2Ce0. 8O1. 9 nanoparticles for reversible solid oxide cells, *International Journal of Hydrogen Energy* 47(2), 747-760.

[12] S.P. Jiang. (2006). A review of wet impregnation—an alternative method for the fabrication of high performance and nano-structured electrodes of solid oxide fuel cells, *Materials Science & Engineering A* 418(1-2) ,199-210.

[13] W.H. Kan, A.J. Samson, V. Thangadurai. (2016). Trends in electrode development for next generation solid oxide fuel cells, *Journal of Materials Chemistry* A 4(46) , 17913-17932.

[14] D. Ding, X. Li, S.Y. Lai, K. Gerdes, M. Liu. (2014). Enhancing SOFC cathode performance by surface modification through infiltration, *Energy & Environmental Science* 7(2) , 552-575.

[15] T. Hong, K. Brinkman, C. Xia. (2016). Copper oxide as a synergistic catalyst for the oxygen reduction reaction on La0. 6Sr0. 4Co0. 2Fe0. 8O3−δ perovskite structured electrocatalyst, *Journal of Power Sources* 329 ,281-289.

[16] C. Gao, Y. Liu, K. Xi, S. Jiao, R. Tomov, R.V. Kumar. (2017). Improve the catalytic property of La0. 6Sr0. 4Co0. 2Fe0. 8O3/Ce0. 9Gd0. 1O2 (LSCF/CGO) cathodes with CuO nanoparticles infiltration, *Electrochimica Acta* 246, 148-155.

[17] Y. Tan, S. Gao, C. Xiong, B. Chi. (2020) .Nano-structured LSM-YSZ refined with PdO/ZrO2 oxygen electrode for intermediate temperature reversible solid oxide cells, *International Journal of Hydrogen Energy* 45(38), 19823-19830.

[18] T.Z. Sholklapper, V. Radmilovic, C.P. Jacobson, S.J. Visco, L.C. De Jonghe. (2008). Nanocomposite Ag–LSM solid oxide fuel cell electrodes, *Journal of Power Sources* 175(1) ,206-210.

[19] S.V. Seyed-Vakili, A. Babaei, M. Ataie, S. Heshmati-Manesh, H. Abdizadeh. (2018). Enhanced performance of La0. 8Sr0. 2MnO3 cathode for solid oxide fuel cells by co-infiltration of metal and ceramic precursors, *Journal of Alloys and Compounds* 737, 433-441.

[20] H.H. Lim, E. Sulistya, M.Y. Wong, B. Salamatinia, B. Amini Horri. (2017). Ceramic nanocomposites for solid oxide fuel cells, Sol-gel Based Nanoceramic Materials: Preparation, Properties and Applications, Springer, pp. 157-183.

[21] C. Knöfel, H.-J. Wang, K.T. Thydén, M. Mogensen. (2011). Modifications of interface chemistry of LSM–YSZ composite by ceria nanoparticles, *Solid State Ionics* 195(1) , 36-42.

[22] N. Imanishi, R. Ohno, K. Murata, A. Hirano, Y. Takeda, O. Yamamoto, K. Yamahara. (2009) .LSM-YSZ Cathode with Infiltrated Cobalt Oxide and Cerium Oxide Nanoparticles, *Fuel Cells* 9(3) 215-221.